Surface Science 261 (1992) 123–128
North-Holland

surface science

X-ray reflectivity study of the Si(111)7 × 7 surface

I.K. Robinson and E. Vlieg [1]
AT&T Bell Laboratories, Murray Hill, NJ 07974, USA

Received 22 July 1991; accepted for publication 16 August 1991

We have measured the X-ray reflectivity profile of the clean 7 × 7 reconstructed surface of Si(111) from small momentum transfer to beyond the (333) reflection of the bulk. The vertical structure is thereby determined to an accuracy of about 0.03 Å. While this result is completely consistent with the dimer-adatom-stacking fault (DAS) model of Takayanagi et al., it disagrees somewhat on the exact positions of the layers determined by LEED, RHEED and X-ray standing waves. The absolute position of the surface layers relative to the distant bulk naturally emerges from the analysis and shows a significant expansion, a result which agrees with a local density approximation theoretical calculation, but differs from the results of these previous experiments.

The 7 × 7 structure of the clean Si(111) surface has been studied exhaustively over a period of 25 years, and the validity of the dimer-adatom-stacking fault (DAS) model of Takayanagi et al. [1] proposed in 1985 is no longer questioned seriously. Much is to be learned, however, from detailed measurements of atomic positions within the DAS framework and this work is still in progress, with recent contributions from low energy electron diffraction [2] (LEED), reflection high energy electron diffraction [3] (RHEED) and in-plane X-ray diffraction [4]. As more accurate positions become available, more of the subtle roles of strain and variations in local coordination can be explored [5]. Until now there is no accurate total energy calculation and coordinate optimization of the 7 × 7 structure because the size of such a project is too large for present day computers, and even this might not answer all the structural questions: the penetration of the strain fields far inside the bulk, for example.

LEED and to a lesser extent RHEED suffer an important drawback from the limited penetration of electrons into the sample. The positions of deeper layers are determined with progressively less and less accuracy, and the vertical position of the surface with respect to the distant bulk is not obtained at all. This aspect of the structure was addressed by a clever differential X-ray standing wave (XSW) experiment [6] in which the different escape depths of KLL and LVV Auger electrons was used for surface sensitivity. A 0.5 Å contraction of the outermost layers was found. The experimental technique was later questioned however and found to suffer from severe artifacts [7]. The question of absolute position has important consequences for the surface stress, that probably affects the energetics of the reconstruction [5,8,9].

The technique of X-ray reflectivity is the X-ray analogue of LEED or RHEED measurements of the (00) specular rod. Any of these techniques is inherently sensitive to the positions of all the layers of the crystal inside the penetration depth and will detect deviations from ideal layer positions wherever they occur within this depth. At the 100 eV electron energy of LEED the depth is only 5 Å, for 10 keV electrons (RHEED) it is 80 Å along the beam direction [10], but for 10 kV X-rays in Si it is more than 1 μm. Thus we can expect to obtain positions most closely referred to the true bulk with X-rays. Another important consequence of the deep penetration is that it arises from a low scattering cross-section, which

[1] Present address: FOM Institute, Kruislaan 407, 1098 SJ Amsterdam, Netherlands.

means the kinematical approximation is rather accurate for X-rays, allowing straightforward analysis by simple one-dimensional Fourier summation over the layers of the crystal. The effects of multiple scattering can be completely neglected. The power of the technique has been elegantly demonstrated for reconstructed surfaces in the recent studies of Au(100) [11].

The importance of accurate knowledge of layer positions, apart from interest in the general phenomenology of oscillatory relaxation and its relation to electronic band structure, is the understanding of the long range distribution of stress forces implied by the observed strain. This can be calculated from the electronic structure and shown to have important effect on the choice of reconstruction present. The variations in bond lengths in a covalent crystal also provide information about the charge redistribution, particularly where adatoms are concerned.

Our experiment was performed on beamline X16A of the National Synchrotron Light Source (NSLS) at Brookhaven National Laboratory using a UHV X-ray diffractometer [12]. The measurements were made with the detector resolution defined by 2×2 mm slits 500 mm from the sample and a beam of 2 mm in height. At small angle the slits were reduced to 1×1 mm and 1 mm respectively to avoid running off the sample, and the data were rescaled. The sample was mounted with the diffractometer axis lying in the surface plane, i.e. 90° away from the usual setting [12]. In this way a large range of momentum transfers was obtained. The sample was prepared by chemical oxidation using the Shiraki [14] method, followed by resistive heating to about 1200 °C to yield a 7×7 LEED pattern.

Data were collected for each point on the reflectivity profile as scans of the diffractometer θ axis sufficiently far to reach background. The peak was numerically integrated and background subtracted. No trend in the shapes of the peaks was observed; they were always resolution-limited. Data were also taken by scanning in the perpendicular χ direction [12] yielding consistent results. Each intensity point was multiplied by $\sin\theta$, the appropriate "Lorentz factor" [13], where θ is the angle of incidence; no polarization correction was needed because of the vertical scattering geometry. A second multiplication by $\sin\theta$ represents the variation of sample area with diffraction angle [13]. Error bars for each point were estimated as a quadrature combination of counting statistics plus a 5% systematic error, found to represent repeated measurements with different alignment, scan direction and slit settings. The full set of measured intensities is shown as the points on fig. 1. The (111) and (333) Bragg peaks of Si are clearly seen as divergences of the intensity; no attempt was made to measure closer to these, since resolution and detector saturation effects would start to become important.

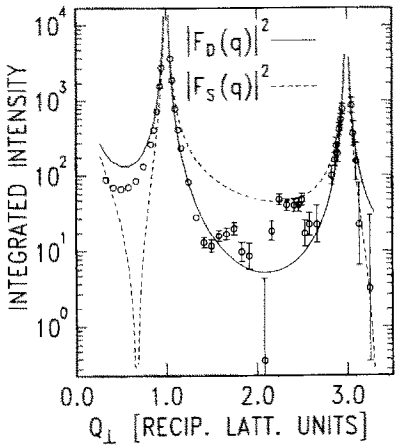

Fig. 1. Measured X-ray reflectivity of the Si(111)7×7 surface. The data points are integrated, background-subtracted and corrected for active area and Lorentz factor. The theoretical curves are attempts to fit eq. (2) and eq. (3), which correspond to the two possible "ideal" terminations of Si(111).

Since Si has the crystal structure of diamond, it has a non-primitive unit cell containing two atoms. This means there are two possible "ideal" terminations (i.e. planar truncation of the bulk) of the (111) surface, case "D" (double layer) with perpendicular dangling bonds and "S" (single layer) with three times the number of bonds at 19° inclination. These are shown in fig. 2.

The calculated reflectivity profile is simply the zero-order crystal truncation rod (CTR) of the lattice [15]. The scattering amplitude can be represented as a one-dimensional sum over the layers of the crystal from the top ($z = 0$) to $z = \infty$. Quite generally we can represent each layer by an

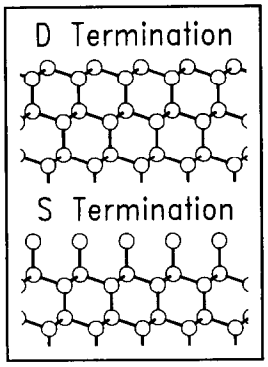

Fig. 2. Ball and stick models of the two possible "ideal" terminations of Si(111).

index j, a position z_j, and a density ρ_j (fractional occupancy between 0 and 1):

$$F(q) = f(q) \sum_{j=0}^{\infty} \rho_j \, e^{iqz_j}, \tag{1}$$

where $f(q)$ is the known form factor for Si, and can be used to include overall scale and Debye–Waller factors as well. Expressions for the amplitude in the two ideal cases "S" and "D" are readily derived:

$$|F_S(q)| = f(q) \frac{\cos(\frac{3}{8}qa)}{\sin(\frac{1}{2}qa)}, \tag{2}$$

$$|F_D(q)| = f(q) \frac{\cos(\frac{1}{8}qa)}{\sin(\frac{1}{2}qa)}, \tag{3}$$

where $a = 3.135$ Å is the Si(111) layer spacing. The calculated intensities, $|F(q)|^2$, are superimposed on the data in fig. 1 after adjusting only scale and Debye–Waller (DW) factors for agreement close to the Bragg peaks.

The reflectivity profile is clearly very sensitive to the choice of termination. This is also a clear demonstration of the importance of structural details on CTRs in general. The $1/|q|^2$ behavior of the intensity close to the Bragg peaks (where $F_D(q)$ and $F_S(q)$ converge) can be predicted from the general form of the Fourier transform of a dielectric boundary [16], but this would have been *independent* of the structure.

The experimental data on the whole fall closer to the $|F_D(q)|^2$ curve than $|F_S(q)|^2$, but do not really agree with either. They in fact appear to oscillate between the two extremes. The oscillations are presumably due to the reconstruction, which must therefore be spread over several layers, since the period is fairly short. As a first attempt to explain these we use eq. (1) with the published parameters taken from the DAS model. The vertical coordinates were taken from the literature [2,3,8,9] and used to calculate an average position z_j, and "thickness" for each layer. The thickness, $\zeta_j = \langle z^2 - z_j^2 \rangle^{1/2}$, is the standard deviation (square root of the second moment) of the distribution of all the atomic height coordinates, z, within the jth layer of the 7×7 unit cell. The many non-equivalent atoms of the reconstruction are thereby reduced to two average layers per bilayer, with two parameters each. The range of momentum transfer (resolution limit) covered by the measurements is appropriate for the refinement of two parameters per layer, but not more, with statistical significance. To include thickness, we modify eq. (1) to the following:

$$F(q) = f(q) \sum_{j=0}^{\infty} \rho_j \, e^{-(1/2)q^2\zeta_j^2} \, e^{iqz_j}. \tag{4}$$

Fig. 3 shows a side view of part of the DAS model that defines the parameterization of the layer positions z_j. Table 1 gives the values for these, derived from the literature by averaging and conversion to common units. The tabulated values are somewhat distorted in the case of the accurate local density approximation (LDA) theory [8] because that only applies to a 2×2 unit

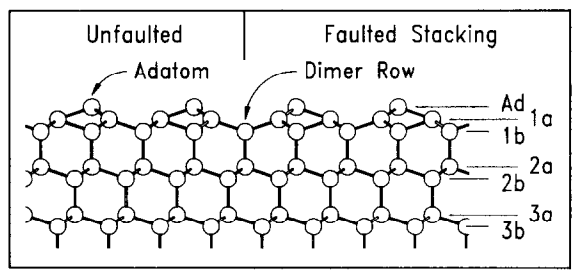

Fig. 3. Ball and stick diagram of the dimer-adatom-stacking fault (DAS) model of the reconstructed Si(111)7×7 surface viewed from the side. All atoms are in unrelaxed "ideal" positions indicated in table 2. The layer notations used in the paper are defined.

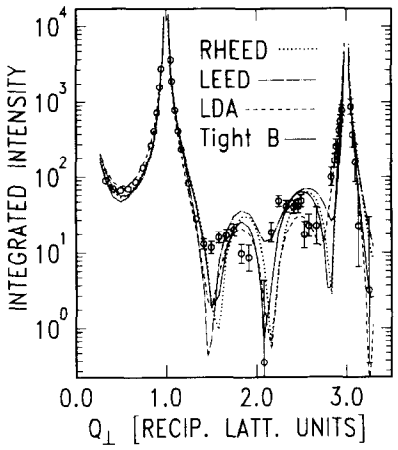

Fig. 4. Reflectivity data with superposition of eq. (4), calculated for four different sets of published vertical coordinates for the DAS model of Si(111)7×7.

cell; the averages then refer to that smaller cell instead. In the case of the RHEED experiment [3], the DAS model was broken into partial layers, with up to three components for each one used here: these were averaged with appropriate weighting. For the LEED [2] and the semi-empirical tight-binding model [9] all coordinates were determined separately.

Eq. (4) was evaluated for each of these models to give the curves drawn over the data in fig. 4. The layer occupancies, ρ_j, were fixed to the values of the DAS model. Three parameters were adjusted in each case: a scale factor, an overall DW factor and an overall roughness factor, β, that gives rise to a q-dependent prefactor [15] in eq. (4). The least-squares residual was evaluated for each model,

$$\chi^2 = \frac{1}{N-P} \sum_{k=1}^{N} \frac{\left(F_k^{\text{obs}} - \left|F_k^{\text{calc}}\right|\right)^2}{\sigma_k^2}, \qquad (5)$$

where P is the number of free parameters and σ_k are the experimental errors in the measurements of F_k. The LDA theory [8] gave $\chi^2 = 8.9$, the RHEED model [3] $\chi^2 = 15.6$, the LEED model [2] $\chi^2 = 13.4$, and the semi-empirical tight-binding calculation [9] $\chi^2 = 11.6$. The curves are fairly similar to each other and to the data, since all have three characteristic minima between (111) and (333), but the positions of the minima are

Table 1
Values of refined layer displacements from ideal DAS positions and layer thicknesses (standard deviations of height distributions) with comparison of previous work (values are in Å and error bars are in parentheses)

Layer name (fig. 3)	Parameter (present work)	Previous experiments		Theoretical calculations	
		RHEED (Ref. [3])	LEED (Ref. [2])	LDA (Ref. [8])	Semi-emp. (Ref. [9])
(a) Layer displacements					
Adatom	0.88 (0.20)	0.38	0.31	0.38	0.44
1a	0.08 (0.03)	−0.07	−0.12	0.02	−0.02
1b	0.02 (0.03)	−0.11	−0.17	0.01	−0.12
2a	−0.04 (0.03)	−0.10	−0.08	−0.02	−0.12
2b	−0.01 (0.03)	0.00	−0.02	0.01	0.00
3a	−0.00 (0.03)	0.00	0.00	−0.00	0.00
3b	−0.00 (0.03)	0.00	0.100	0.00	0.00
(b) Layer thicknesses					
Adatom	0.08 (0.16)	0.00	0.04	0.00	0.03
1a	0.10 (0.09)	0.13	0.06	0.26	0.15
1b	0.09 (0.07)	0.21	0.32	0.28	0.22
2a	0.15 (0.05)	0.18	0.23	0.22	0.20
2b			0.05	0.07	
3a				0.08	

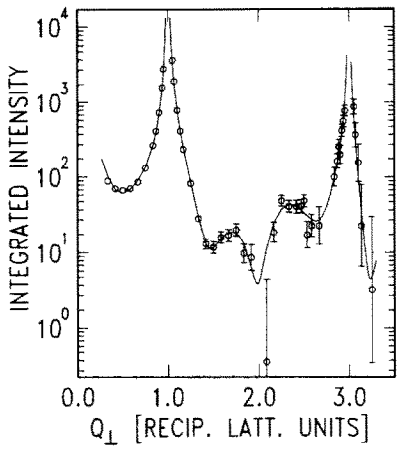

Fig. 5. Refelctivity data with the calculated curve (eq. (4)) for the best refined coordinates of the DAS model of Si(111)7×7.

substantially shifted and result in the rather large values of χ^2.

Refinement of the layer positions and thicknesses to minimize eq. (5) resulted in the curve of fig. 5 and a final $\chi^2 = 0.94$. That this value is of order unity implies there is no further information attainable from the data. The parameters obtained are listed in table 1. Error bars were estimated conservatively as the range of parameter values that retained χ^2 below 2. The scale factor, DW factor and roughness factor, β, were all essentially unchanged from above. The value obtained, $\beta = 0.06 \pm 0.05$, corresponds to an RMS roughness [15] of only 0.01 Å, and is only a small correction to the fit.

The question we set out to answer was the vertical layer positions relative to the bulk lattice deep inside the crystal, to look for accumulated strain. As mentioned above, the previous experimental values were not referenced to the bulk at all, and even the theories are not necessarily correct in this respect because of their finite slab size. The interlayer spacings are derived in table 2. The result we obtain is a slight contraction of the second double layer (layers 2a and 2b) and an expansion of the top layers (1a and 1b). This trend is in agreement only with the results of the LDA calculation. It finds the opposite sign from RHEED [3] and LEED [2] for the change in top layer spacing, and most dramatically contradicts the XSW experiment that reported a large 0.5 Å contraction [6].

The most glaring inconsistency between the best-fit parameters and those determined previously is in the height of the adatom, however. Our Ad–1a spacing is bigger than any of the previous values by 0.3 to 0.4 Å. This results in a bondlength for the adatom backbond of 2.43 Å, longer even than the bulk bondlength of 2.35 Å. We will now dicuss the possible reasons for the discrepancy. In the case of LEED [2] and RHEED [3], the diffracting electron interacts most strongly with the valence electrons, which are strongly distorted for an adatom with all its bonds pointing in the same direction. There is probably considerable charge transfer as well. Stated differently, the phase shift used in the dynamical calculations should be different for an adatom. Similarly the semi-empirical tight-binding calculation required some ad hoc assumptions about the special bonding of the adatom [9]. With so little

Table 2
Values of mean interlayer spacings compared with previous work (values are in Å and error bars are in parentheses)

Spacing (fig. 3)	Ideal value	Present work	Previous experiments		Theoretical calculations	
			RHEED (Ref. [3])	LEED (Ref. [2])	LDA (Ref. [8])	Semi-emp. (Ref. [9])
Ad–1a	0.78	1.58 (0.20)	1.23	1.21	1.14	1.25
1a–1b	0.78	0.85 (0.04)	0.83	0.84	0.80	0.88
1b–2a	2.35	2.41 (0.04)	2.34	2.26	2.37	2.35
2a–b	0.78	0.75 (0.04)	0.68	0.72	0.76	0.66
2b–3a	2.35	2.35 (0.04)	2.35	2.33	2.36	2.35
3a–3b	0.78	0.78 (0.04)	0.78	0.78	0.78	0.78

knowledge of this configuration, a quantitive error could have occurred.

The most disturbing discrepancy is with the LDA calculation, which makes only minimal assumptions, such as the validity of the pseudopotentials, and a suffient choice of reciprocal space cutoff. Two factors deserve mention, however. The calculation is strictly at zero temperature, whereas the adatoms are known to have strong vibration modes at room temperature [17]. To the extent that these vibrations are anharmonic (as is reasonable), a considerable differential thermal expansion could result, that would enlarge the spacing at room temperature. In metals, surface thermal expansion coefficients ten times bigger than the bulk are known [18]. The second point is that the LDA calculation was for a 2×2 unit cell and yields a total energy per unit cell *higher* than the metastable 2×1 π-bonded chain structure [19]. Considerable further relaxation is therefore expected; a mechanism of cooperative relief of strain between the adatoms and dimers of the DAS structure has been proposed [5,20]. Whatever the mechanism, the additional relaxation will most likely result in an increased adatom height.

Finally there is always the possibility that our sample was contaminated. Ohdomari [21] has pointed out that an Ad–1a bond is an excellent target for oxygen attack of Si(111), and has further suggested that oxygen contamination might even be the reason the 7×7 with structure occurs at all. Deliberate attack of Si(111)7×7 oxygen in the presence of an electron beam has shown a preference for this site [22]. To test for this possibility, we allowed the ρ_{Ad} occupancy value to vary, but found no improvement in the fit or any significant increase from the DAS value of 12/49.

NSLS is supported by the US Department of Energy under grant DE-AC012-76CH00016.

References

[1] K. Takayanagi, Y. Tanishiro, S. Takahashi and M. Takahashi, Surf. Sci. 164 (1985) 367.
[2] H. Huang, S.Y. Tong, W.E. Packard and M.B. Webb, Phys. Lett. A 130 (1988) 166.
[3] A. Ichimiya, Surf. Sci. 192 (1987) L893.
[4] I.K. Robinson, W.K. Waskiewicz, P.H. Fuoss and L.J. Norton, Phys. Rev. B 37 (1988) 4325.
[5] I.K. Robinson, J. Vac. Sci. Technol. A 6 (1988) 1966.
[6] S.M. Durbin, L.E. Berman, B.W. Batterman and J.M. Blakely, Phys. Rev. Lett. 56 (1986) 236.
[7] S.M. Durbin and T. Gog, Phys. Rev. Lett. 63 (1989) 1304.
[8] R.D. Meade and D. Vanderbilt, Phys. Rev. B 40 (1989) 3905.
[9] G.X. Qian and D.J. Chadi, Phys. Rev. B 35 (1987) 1288.
[10] From the "universal curve" of electron mean free paths, see for example: G. Ertl and J. Küppers, Low Energy Electrons and Surface Chemistry (Verlag Chemie, Weinheim, 1974).
[11] D. Gibbs, B.M. Ocko, D.M. Zehner and S.G.J. Mochrie, Phys. Rev. B 38 (1988) 7303.
[12] P.H. Fuoss and I.K. Robinson, Nucl. Instrum. Methods 222 (1984) 171.
[13] E. Vlieg, A.W. Denier van der Gon, J.F. van der Veen, J.E. Macdonald and C. Norris, Surf. Sci. 210 (1989) 301.
[14] A. Ishizaka, N. Nakagawa and Y. Shiraki, in: Proc. 2nd Int. Symp. on MBE and Related Clean Surface Techniques (JSAP, Tokyo, 1982) p. 183.
[15] I.K. Robinson, Phys. Rev. B 33 (1986) 3830.
[16] M. van Laue, Ann. Phys. 26 (1936) 62;
S.R. Andrews and R.A. Cowley, J. Phys. C 18 (1985) 6427.
[17] W. Daum, H. Ibach and J.E. Müller, Phys. Rev. Lett. 59 (1987) 1593.
[18] Y. Cao and E.H. Conrad, Phys. Rev. Lett. 65 (1990) 2808.
[19] D. Vanderbilt, Phys. Rev. Lett. 59 (1987) 1456.
[20] M.C. Payne, J. Phys. C 20 (1987) L983.
[21] I. Ohdomari, Surf. Sci. 227 (1990) L125.
[22] J.M. Gibson, Surf. Sci. 239 (1990) L531.